Hindawi
Shock and Vibration
Volume 2018, Article ID 1879392, 16 pages
https://doi.org/10.1155/2018/1879392

Research Article

Vibration Induced by Subway Trains: Open-Trench Mitigation Analysis in the Time and Frequency Domains

Wenbo Yang,[1] **Ran Yuan**,[1] **and Juan Wang**[2]

[1]*Key Laboratory of Transportation Tunnel Engineering, Southwest Jiaotong University, Ministry of Education, Chengdu, China*
[2]*Ningbo Nottingham New Materials Institute, The University of Nottingham Ningbo, Ningbo, China*

Correspondence should be addressed to Ran Yuan; yuanran@swjtu.edu.cn

Received 2 March 2018; Revised 3 July 2018; Accepted 2 August 2018; Published 3 September 2018

Academic Editor: Lutz Auersch

In this paper, we analyse the mitigation effects of open trenches on the vibrations induced by subway trains. The study is performed by using both physical model tests and numerical simulations. The effectiveness is evaluated by calculating the frequency response function (FRF) and the vibration acceleration peak (VAP) in both time and frequency domains. The experimental and numerical results demonstrate that the open trench has clear effects on the dynamic soil response. Both time and frequency domain results suggest that the dynamic response of the soils beyond the open trenches could be significantly affected, due to the existence of the open trench. According to the frequency domain analysis, the inclusion of open trenches could effectively reduce the soil response in a higher frequency range. Due to reflection effects at the boundaries of the trench, an amplification of the soil response in front of the open trench is observed. Parametric study by means of numerical simulations is also performed. The width of the open trench demonstrates negligible effects on the dynamic soil response, whilst the trench depth exhibits a large influence on the trench isolation performance. With an increase in the trench depth, the isolation performance is significantly improved. It is concluded that the open trenches perform well as an isolation barrier, in mitigating the vibration induced by subway trains.

1. Introduction

The rapid extension and extensive use of trains have enhanced the convenience of public transportation significantly. However, the vibrations that are generated by rail traffic can cause significant problems. They can cause distress to people who live near the rails, and they can threaten nearby structures that house sensitive machinery. Vibrations could propagate from the tunnels to nearby buildings. This can cause a perceptible vibration as well as reradiated noise which may have a significant impact on the comfort of residents of buildings [1].

Many vibration countermeasures have been developed to reduce the vibration effects from railways. Various types of isolation are discussed in the literature, e.g., open and filled trenches, concrete walls or piles, and flexible gas cushions [2–7]. Among these types of isolation, the open trench has been demonstrated as an effective intervention, and it is the most common intervention in practical traffic applications, especially for mitigating vertical vibrations [6]. There are mainly two reasons that open trenches can be an effective way to mitigate the vibration transmitted from the soil to buildings, i.e., (1) they are one of the lowest cost isolation measures [8], (2) they provide better vibration reduction capacity [9–12].

In the past, efforts were made to use open trenches to analytically and experimentally solve vibration reduction problems. Closed-form solutions [13, 14] were obtained, and model tests for particular cases [15–17] were conducted, but they were restricted to simple geometries and idealized problems. To complement the analytical and experimental studies, numerical simulations have been used extensively to investigate the performance of open trenches because they can be used to analyse complicated geometries and conditions. Hence, it is possible to provide design guidelines for practical traffic applications. Two-dimensional (2D) Finite Element (FE) models were established by May and Bolt to analyse the influence of open trenches on various types of incident waves [18]. Ahmad and Al-Hussaini conducted 2D boundary element (BE) simulations to study the performance of trench barriers with various

geometrical and material parameters [12]. Coupled finite/infinite methods (e.g., [19]), finite difference methods (e.g., [20]), and coupled FE/BE methods (e.g., [8, 21–23]), varying from two-dimensional models to 2.5-dimensional cases, have been used by many authors to study the effectiveness of open trenches in reducing vibrations. Different types of the grounds, i.e., homogeneous grounds [24, 25] and nonhomogeneous grounds [11, 26], have been analysed. More recently, high-speed railways have attracted a lot of attention, and several studies have been conducted to investigate the use of trenches as vibrating attenuating barriers for the mitigation of vibrations [27, 28].

Although the effectiveness of open trenches for mitigating train-induced vibrations generally has been recognized, as mentioned above, most published results have concentrated on the ground-borne vibrations induced by trains running on surface railways. However, subway trains have become much more prevalent in urban areas, especially in densely populated cities. Several empirical procedures have been proposed for estimating the level of ground-borne vibration due to subway trains [29–31], but their scope is rather limited. Sheng et al. pointed out that the oscillation frequencies induced and transmitted by subway trains via propagation through the ground are in the range of 15–200 Hz [32]. Thompson et al. have agreed that subway trains induce higher frequency vibrations at considerably lower amplitudes than trains on surface railways, and this ground-borne noise has a greater adverse effect on the sound inside buildings [33]. Field data have indicated that vertical ground vibration is more important than the horizontal ground vibration induced by subway trains [34, 35]. Although open trenches are effective at attenuating vibrations that propagate in the vertical direction, few studies have been performed to analyse the effectiveness of open trenches in mitigating the vibrations caused by subway trains.

In our study, both physical model tests and numerical simulations are used to evaluate the effectiveness of open trenches for mitigating the vibrations induced by subway trains. We investigate cases with and without open trenches. We analyse the effectiveness of open trenches for mitigating the dynamic response of the soils surrounding the subway tunnels, in the time and frequency domains. The effects of vibration frequencies on the trench isolation performance are examined. Parametric studies are performed to determine the critical case with best vibration isolation effects, by means of numerical simulations.

2. Model Tests

Physical model tests have been conducted in this study. Due to the fact that the dynamic force from an underground tunnel can be relatively small, the behavior of soils would usually remain within the linear range [36–39]. Thus, an elastic scaling law was used. Elastic scaling laws were determined according to Iai, 1989 [40] and Iai et al., 2005 [41]. Three fundamental scaling factors, i.e., geometry, density, and Young's modulus, were 1/20, 1/1, and 1/30, respectively. Other relative parameters were altered based on the elastic scaling law, as detailed in Table 1.

Table 1: Model scaling of physical parameters.

Parameters	Scaling factor	Model/Prototype
Length	C_l	1/20
Density	C_ρ	1/1
Young's modulus	C_E	1/30
Force	$C_F = C_l^3 \cdot C_\rho$	1/8000
Strain	$C_\varepsilon = C_l \cdot C_\rho \cdot C_E^{-1}$	1/0.667
Stress	$C_\sigma = C_E \cdot C_\varepsilon$	1/20
Acceleration	$C_a = a_m / a_p$	1/1
Velocity	$C_v = C_E^{0.5} \cdot C_\rho^{-0.5}$	1/5.477
Displacement	$C_u = C_l \cdot C_\varepsilon$	1/13.333
Dynamic time	$C_t = C_l \cdot C_\rho^{0.5} \cdot C_E^{-0.5}$	1/3.651
Frequency	$C_\omega = C_t^{-1}$	1/0.274

2.1. Test Facilities. The experiments were performed using a steel model box with effective length, width, and height dimensions of 1.5 m, 0.9 m, and 1.35 m, respectively [42]. Any undesirable reflections of the compressional wave and shear wave from the rigid boundaries of the steel box could reduce the accuracy of the test results. To eliminate boundary effects, an energy absorbing material, i.e., Duxseal (30 mm thick), was installed on the bottom and side walls of the box to absorb incident waves [43–46]. The test model was mainly composed of a subway tunnel and the surrounding soil layer (Figure 1). The typical subway tunnel was modelled as a prototype in the experimental tests, and the corresponding diameter and lining thickness were 5.7 m and 0.3 m, respectively. The model subway tunnel was supported by a segment lining that had an inner diameter of 270 mm. Each segment was 15 mm thick and 75 mm wide. For the construction of the lining of the segment, we believed that controlling its overall bending moment characteristics was one of the most significant problems, so this aspect was given careful consideration in the design of the lining. We used the staggered joint method in the assembling mode in order to control the design values of the positive and negative moments, the shearing force of the lining, and the shearing forces of the longitudinal bolts in the universal segment lining. Each ring of the segment lining contained three standard blocks, i.e., two abutment blocks and one block to seal the roof. A 9 mm groove was made in which the longitudinal joints were placed to reduce the bending stiffness; hence, the bending characteristics of the model joint were consistent with those of its corresponding prototype [47]. The longitudinal joint was represented by a series of steel sticks with diameters of 4 mm. The transverse shear stiffness was assumed to be infinite, because any sliding between the adjacent segments was ignored due to the few deformations of the structure of the tunnel [42]. Two series of experiments were conducted to examine the isolation performance of the open trench. Figure 2(a) shows the model without an open trench, whilst the model with an open trench is shown in Figure 2(b). The length, width, and height of the open trench were 800 mm, 100 mm, and 900 mm, respectively. The right-side boundary of the open trench was 40 cm from the vertical centerline of the subway tunnel.

The subway soil formation prototype consisted of homogeneous soft soils. In this study, a uniform soil layer was modelled. To satisfy the scaling laws of the test, a mixed material of quartz sand, coal ash, river sand, and oil was used

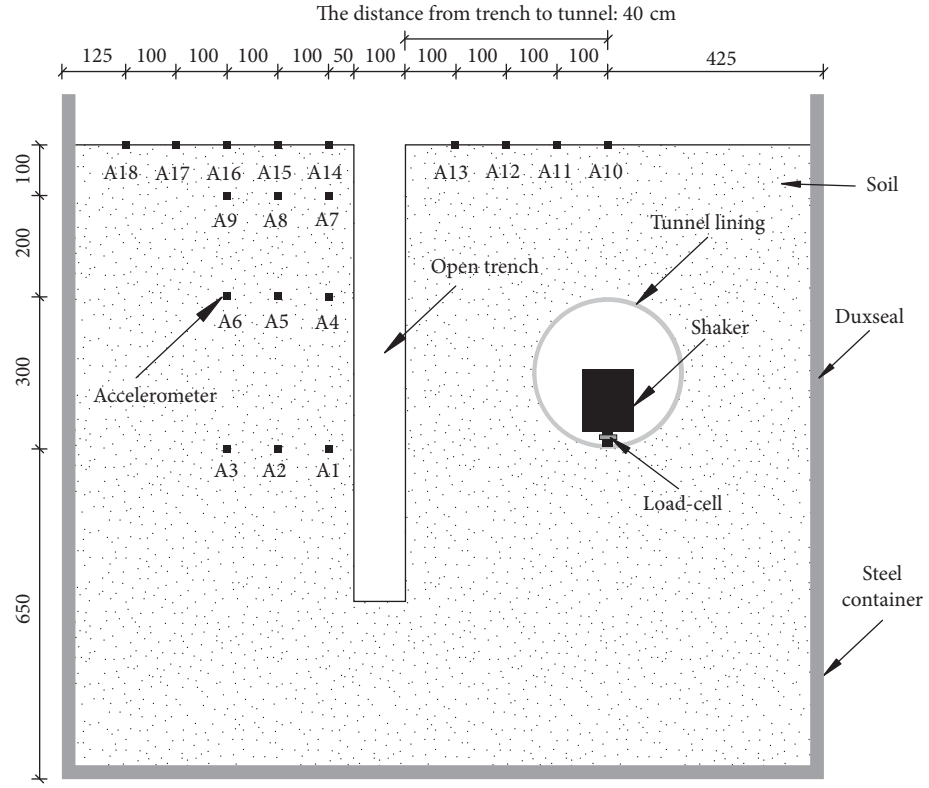

Figure 1: Acceleration sensor layout (mm).

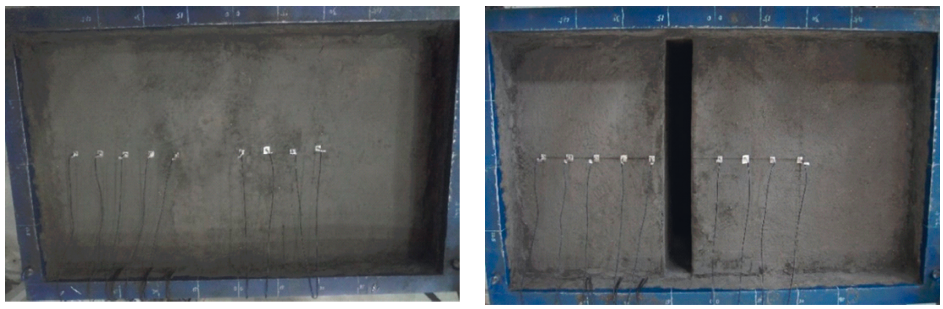

(a) (b)

Figure 2: Test conditions: (a) without the open trench; (b) with the open trench.

as tested soils (the corresponding mass ratio is 54 : 27 : 12 : 7, respectively) [42]. The lining segments of the subway tunnel were modelled by a mixture of diatomite, plaster stone, and water (the corresponding mass ratio is 0.4 : 1.0 : 1.8) [48]. Uniaxial compression tests were conducted to determine the mechanical parameters of the model lining and soil. By varying the amount of components of the mixed material, different elastic parameters can be obtained, as shown in Table 2. The material properties of the soils and lining segments for the prototype and the testing model have been presented in Tables 3 and 4, respectively. The soils were poured into the steel box from a constant height at a constant velocity in order to ensure the uniformity of the soil and to control its density [46, 49].

To simulate the excitation caused by a subway train, we used an electromagnetic dynamic shaker (type JM-20) in the tests. Figure 3 shows that the shaker was placed vertically at the bottom of the tunnel lining to provide a vertical dynamic excitation at the center of the tunnel invert. In order to apply the dynamic load accurately, the shaker worked in conjunction with a JM-1230 wave generator and a corresponding JM5801 power amplifier. A JM0710-001 washer-shaped dynamic load cell was used to measure the force from the shaker. Eighteen JM0213 piezoelectric accelerometers were placed at the free surface, and accelerometers were also installed in the interior of the soil layer adjacent to the open bench, to measure the dynamic response of the model. The vertical vibration component is most commonly representative of the vibration field. In addition, the horizontal component could be hard to measure due to the limitations of the instruments and technologies. Due to the two reasons, the vertical vibration has been measured and recorded in the

Table 2: Material ratios of mixed material and mechanical parameters of tunnel lining.

Numbering	Material ratio			Elastic modulus (GPa)	Compressive strength (MPa)
	Water	Plaster stone	Diatomite		
1	2	1	0.1	0.84	0.365
2	2	1	0.2	0.732	0.765
3	2	1	0.3	0.75	0.87
4	2	1	0.4	0.905	1.325
5	2	1	0.5	1.11	1.31
7	2.1	1	0.4	0.95	1.045
8	2.2	1	0.4	0.73	0.865
9	2.3	1	0.4	0.695	0.81
10	1.9	1	0.4	1.225	1.43
11	1.8	1	0.4	1.1	1.47
12	2.4	1	0.4	0.63	0.61

Table 3: Properties of the soils.

	Density (kg/m^3)	Elastic modulus (MPa)	Shear modulus (MPa)	Poisson's ratio, μ
Prototype	2000	60	23.08	0.3
Model	2000	2	0.77	0.3

Table 4: Material properties of the lining segments.

	Density (kg/m^3)	Elastic modulus (GPa)	Shear modulus (GPa)	Poisson's ratio, μ
Prototype	2400	34.5	13.3	0.3
Model	2400	1.1	0.44	0.3

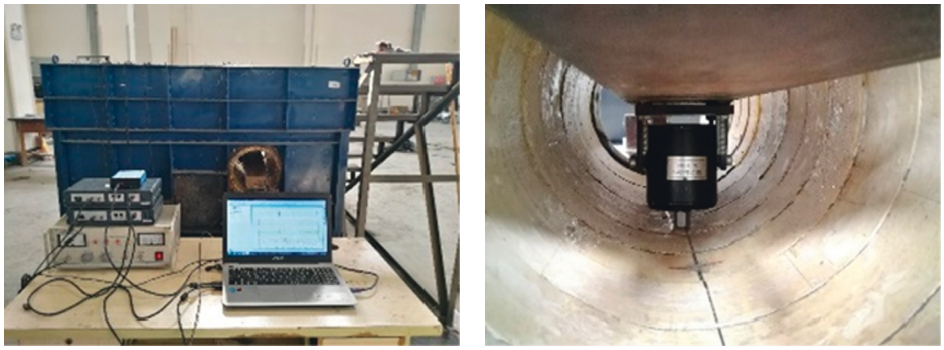

(a) (b)

Figure 3: Model test equipment: (a) control system; (b) shaker.

present experimental tests. Figure 1 shows that testing points A10–A13 were located in front of the open trench, while the other testing points were located beyond the open trench.

2.2. Test Performance. Two series of experiments were performed, one with the open trench and one without. Three kinds of dynamic forces were applied on the tunnel invert during each test, i.e., harmonic loading, sweep loading, and train-induced vibration loading. During the experiment, firstly, three types of vibration signals were generated in the JM-1230 type wave generator and then passed to the corresponding JM5801 power amplifier. Then, the amplified vibration signal was sent to the JM-20 electromagnetic shaker to vibrate the model subway tunnel. In order to record the data accurately, a sampling frequency of 8000 Hz was chosen, approximately 10 times to the maximum frequency component of the measured signal.

At the first instance, the harmonic loading was applied so that the results of the test could be compared directly with the numerical results in order to validate the numerical formulation and solution procedures. Figure 4(a) shows an example of the harmonic signal in which the fixed frequency was 200 Hz (prototype scale). In order to study the isolation performance of the open trench at various vibration frequencies, we used a sweep sinusoidal frequency with a period of 5 seconds (Figure 4(b)), covering the entire frequency domain induced by the subway train, which varied from 0 Hz to 200 Hz (prototype scale). Figure 4(c) shows the frequency domain of the sweep frequency load.

The induced vibration load of the train was also used in the experimental test. According to the existing research

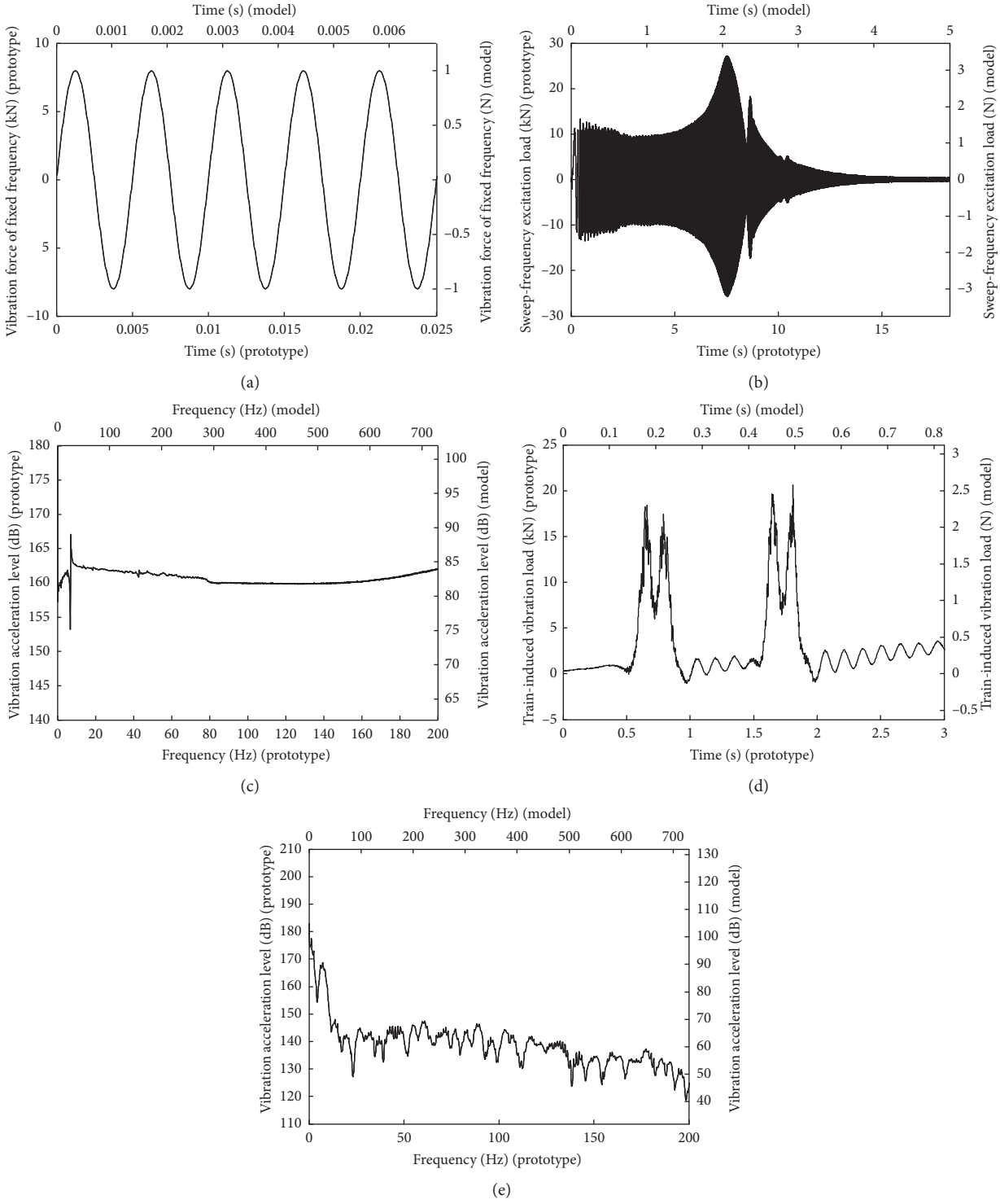

Figure 4: Dynamic loads applied in the experiment. (a) Sinusoidal loads at a fixed-frequency 200 Hz (prototype scale). (b) Sweep loads in time domain. (c) Sweep loads in frequency domain. (d) Train loads in time domain. (e) Train loads in frequency domain.

results [50, 51], we established a three-dimensional model that coupled the vehicle and the track. The vibration load caused by irregularities in the track emphatically was considered. The train load of two track spectra (level 5 and level 6) and three speeds (40, 50, and 60 km/h) was obtained. In this paper, we used the train load of the level 5 track spectrum, the speed limit of which was 60 km/h. Figure 4(d) shows the typical subway-induced vibration loads, and Figure 4(e) shows the frequency domain of the train load. When the train was passing through the subway tunnel, the effects of the open trenches on the vibration acceleration peaks (VAPs) of the test points have been evaluated in the time domain.

3. Numerical Simulations

The finite difference software Fast Lagrangian Analysis of Continua (FLAC^{3D}) was used to perform the numerical simulations and to compare with the model tests. The three-dimensional FLAC^{3D} model was designed to replicate, as closely as possible, the scale of the dimensions of the prototype used in the model tests. A rectangle was used to model the soil medium, and a horizontal cylinder was buried in it to model the tunnel, as shown in Figure 5. The length, width, and height dimensions of the rectangle were 30 m, 18 m, and 27 m, respectively. The open trench was also modeled by a rectangle that was buried in the soil medium next to the subway tunnel. There was a distance of 9 m between the centerline of the trench and the vertical centerline of the tunnel. The tunnel in the numerical model was designed to coincide with the dimensions of the prototype experimental tunnel, with an outer diameter of 6.0 m, a lining thickness of 0.3 m, and a length of 18 m. The size of the elements in the mesh of the model was less than 1/10 to 1/8 of the corresponding wavelength of the vibration, with 2,000,000 meshed elements [52]. Quiet boundaries [53], which were used to absorb incident waves at the boundaries of the model, simulated an infinite medium. The quiet-boundary scheme proposed by Lysmer and Kuhlemeyer [54] involved dashpots attached independently to the boundary in the normal and shear directions. The dashpots provided viscous normal and shear tractions given by

$$t_n = -\rho C_P v_n, \quad t_s = -\rho C_s v_s, \tag{1}$$

where v_n and v_s are the normal and shear components of the velocity at the boundary; ρ is the mass density; and C_P and C_s are the pressure and shear wave velocities.

The fixed boundary (at the bottom) represented the restraint of the displacements in all three coordinate directions (x, y, and z). A model made of an elastic material was used because the deformation induced by the train was relatively small [55, 56].

A harmonic load at a single frequency was applied at the tunnel invert. By varying the frequency of the harmonic load (from 0 to 200 Hz), we measured the vertical acceleration of the soil surrounding the tunnel with and without an open trench.

Rayleigh damping was taken as the damping model in this study, and the equation of motion is given as

$$C = \alpha M + \beta K, \tag{2}$$

where M and K denote the mass matrix and the stiffness matrix, respectively, α and β denote the mass damping coefficient and the stiffness damping coefficient, respectively.

Two parameters were used to define Rayleigh damping in FLAC^{3D}, i.e., the center frequency and the fraction of critical damping. The center frequency was set to be consistent with the vibration frequency that existed at the tunnel invert. The fractions of critical damping were set as 0.1 and 0.05 for the lining of the tunnel and soil medium, respectively.

A harmonic load at a single frequency with an amplitude of 1 N was applied at the centerline of the numerical tunnel invert ($x = 0$ m, $y = 9$ m, $z = 0.3$ m). The amplitudes of the model's responses at the imposed loading frequency were recorded after the model reached the steady state. By varying the frequency of the harmonic load (i.e., from 0 to 200 Hz), the vertical dynamic responses of the surrounding soil, for cases with or without an open trench, were calculated at the same testing points that were used in the tests of the model. In the parametric studies, the train load was applied at the centerline of the tunnel invert. Vertical peak particle acceleration of soil at ground surface was calculated to study the effect of trench dimensions on vibration mitigation effect.

4. Results and Discussions

The comparison between the experimental and numerical results is performed, for the case of the first instance of harmonic loading, to validate the numerical formulation and the procedures used to obtain the solution. The FRFs and VAPs are calculated and evaluated in order to analyze the effectiveness of the open trench for different sweep frequencies.

4.1. Dynamic Response of Soils Undergoing Harmonic Loading. Figure 6 shows the dynamic responses of the soil for A1, A4, A13, and A14 during the harmonic loading at fixed frequencies of 50 Hz, 100 Hz, and 200 Hz obtained from experimental testing and from numerical simulation. The red curve represents the case with an open trench, and the black curve represents the case without an open trench. Figure 6 shows that the numerical results (dashed lines) and the experimental results (solid lines) are almost identical. Only a small difference occurs at the peak acceleration, which could be because the material parameters that are used as inputs to the numerical model do not exactly represent the model tunnel and the soil.

By comparing the two cases, i.e., with and without an open trench, it is apparent that the open trench provides attenuation for the propagation of vibrations. This attenuation is also observed for the soils beyond the open trench, as shown in Figures 6(a), 6(c)–6(e), 6(g)–6(i), 6(k), and 6(l). For example, at the fixed frequency of 200 Hz, the amplitude of the attenuation of A14 is 68%. This result demonstrates that the open trench efficiently isolates the vibration isolation, and Woods [15] has concluded that a reduction of 0.25 should be considered as "effective." The reason for this observation is that the open trench can interrupt the path in the soil along which the vibration is propagating, so it can effectively reduce the dynamic response of the soil behind the trench. With respect to the soils in front of the open trench (measurement point A13), the dynamic responses of these soils are amplified, with an increase of 24% in at the fixed frequency of 200 Hz. The amplification of the vibration in the soil occurs because reflection waves are generated at the boundaries of the trench, and these waves can propagate back to the ground, resulting in increasing the response of the soil.

4.2. Dynamic Response of Soils to Sweep Loading. The measured time domain data are transferred to the frequency

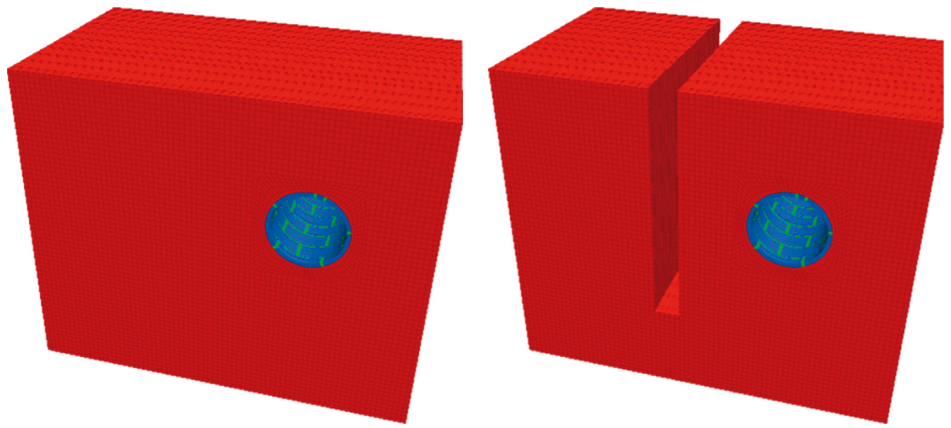

(a) (b)

Figure 5: Illustration of the numerical model: (a) without the trench; (b) with the trench.

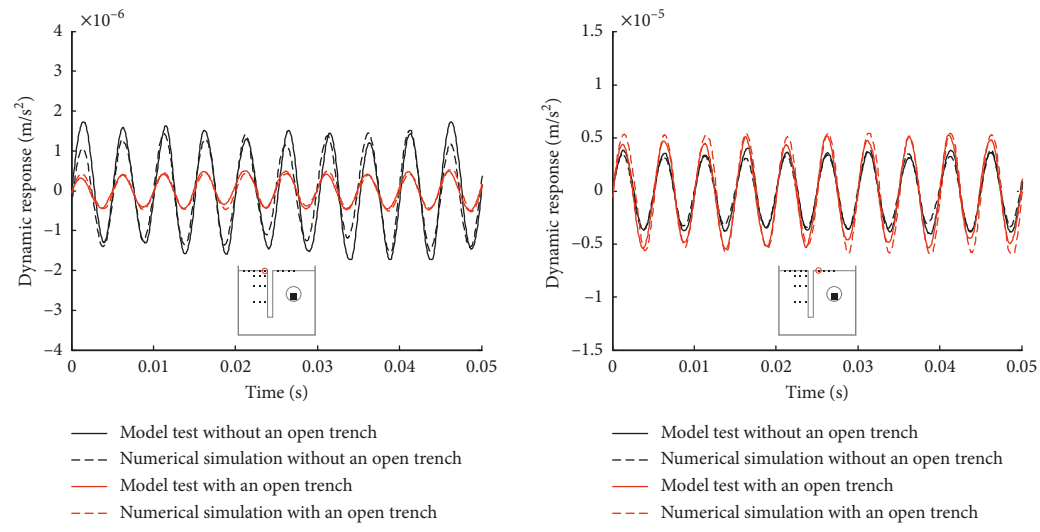

Figure 6: Continued.

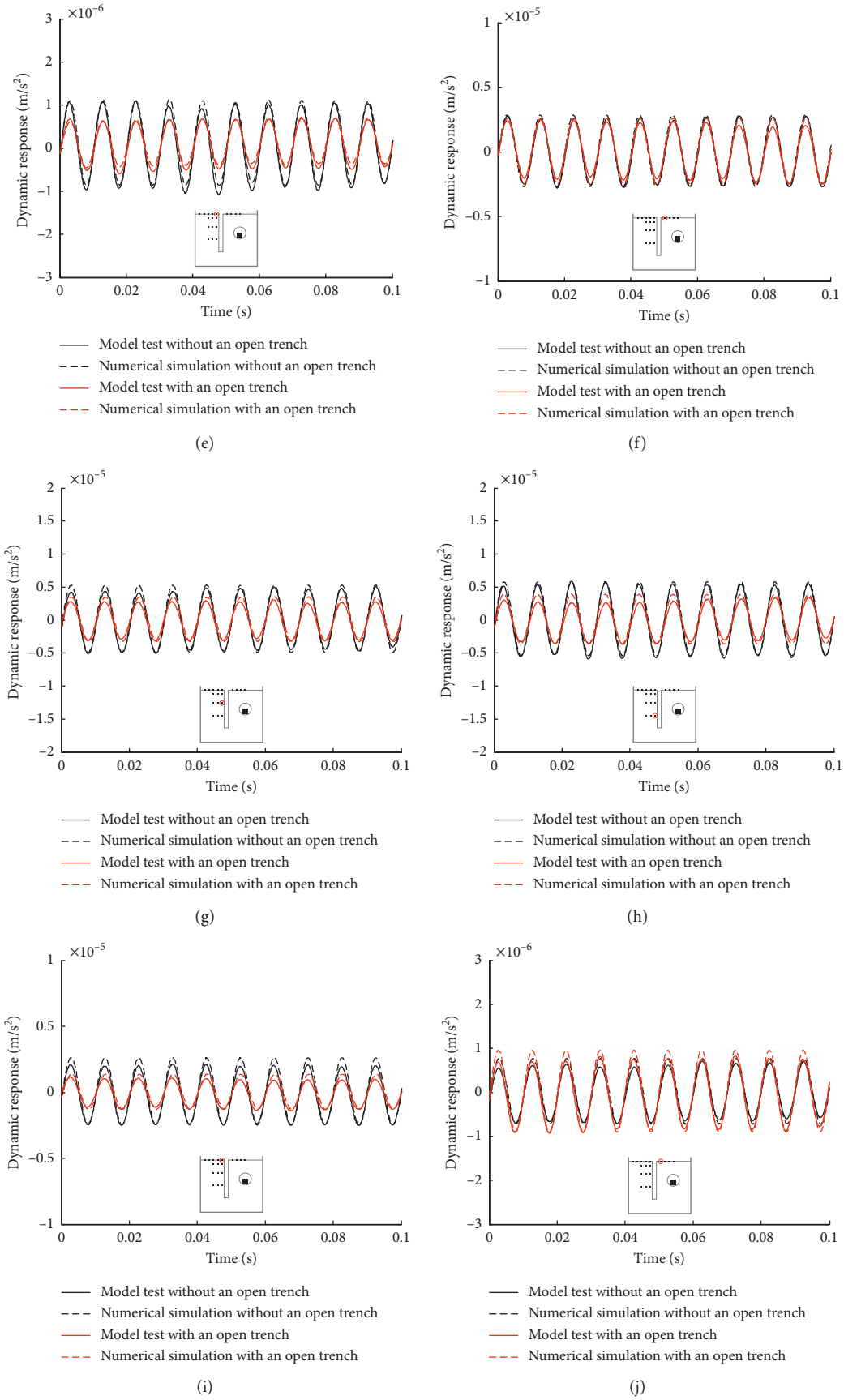

Figure 6: Continued.

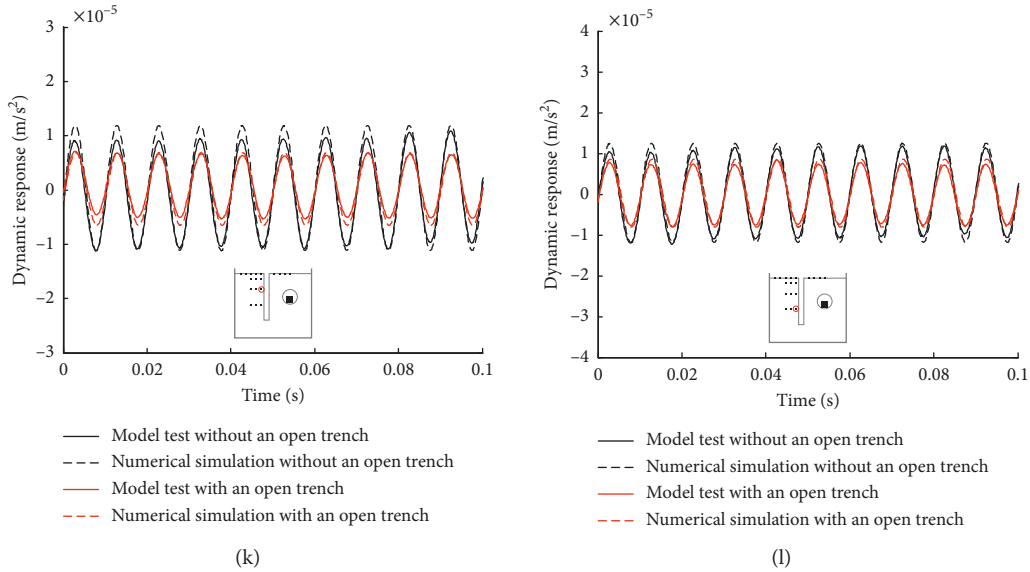

Figure 6: Dynamic response of soils under the action of harmonic loads. (a) 200 Hz at point A14. (b) 200 Hz at point A13. (c) 200 Hz at point A4. (d) 200 Hz at point A1. (e) 100 Hz at point A14. (f) 100 Hz at point A13. (g) 100 Hz at point A4. (h) 100 Hz at point A1. (i) 50 Hz at point A14. (j) 50 Hz at point A13. (k) 50 Hz at point A4. (l) 50 Hz at point A1.

domain, and the FRFs of the model's responses are calculated. The coherence functions, which are used to examine the quality of the FRF measurements, are also calculated and analysed. The FRFs and corresponding coherence functions are

$$\mathrm{FRF}(\omega) = \frac{S_{\mathrm{FA}}(\omega)}{S_{\mathrm{FF}}(\omega)}, \qquad \mathrm{Coh}(\omega) = \frac{S_{\mathrm{FA}}(\omega) S_{\mathrm{AF}}(\omega)}{S_{\mathrm{FF}}(\omega) S_{\mathrm{AA}}(\omega)}, \tag{3}$$

where ω is the frequency, $S_{\mathrm{FF}}(\omega)$ is the autospectrum of the force, $S_{\mathrm{AA}}(\omega)$ is the autospectrum of the response in acceleration, $S_{\mathrm{FA}}(\omega)$ is the cross spectrum of the force and acceleration response, and $S_{\mathrm{AF}}(\omega)$ is the cross spectrum of the acceleration response and force [41, 57, 58].

Figure 7 shows the experimental results of values of the coherence function for testing points A1, A4, A7, A10, A13, and A14 without the open trench, and it shows that the values of the coherence function are close to 1 when the excitation signal is larger than 50 Hz. A coherence value of 1 indicates that the measured response is 100% due to the measured excitation. However, when the excitation signal ranges from 0 Hz to 50 Hz, the values of the coherence function generally are less than 0.8. As mentioned earlier, this may due to the effects of unwanted noise, which are proportionately higher when the magnitude of the measured signal is low. Hence, only numerical simulations are used to investigate the vertical dynamic response of soils when the measured signal is low (i.e., less than 50 Hz).

Figures 8 and 9 show the numerical and experimental results, respectively, of the FRFs of the vertical dynamic soil responses that correspond to the surface measurement points beyond and in front of the open trench. The frequency domain results are presented in prototype scale because, in

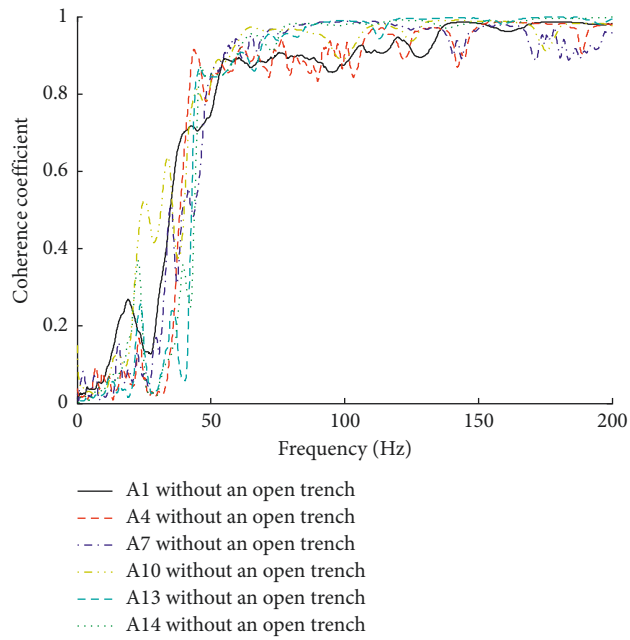

Figure 7: Coherence coefficient at points A1, A4, A7, A10, A13, and A14.

that case, the model's results can be compared directly with the numerical results. The red curves represent the case with an open trench, and the black curves represent the case without an open trench. The solid curves represent the test results of the physical model, and the scattered plots represent the numerical simulation.

Figures 8 and 9 show that, generally, a reasonably good match of the experimental and numerical results can be obtained. The average difference is within 5 dB, which may due to the effect of unwanted noise (mainly due to the

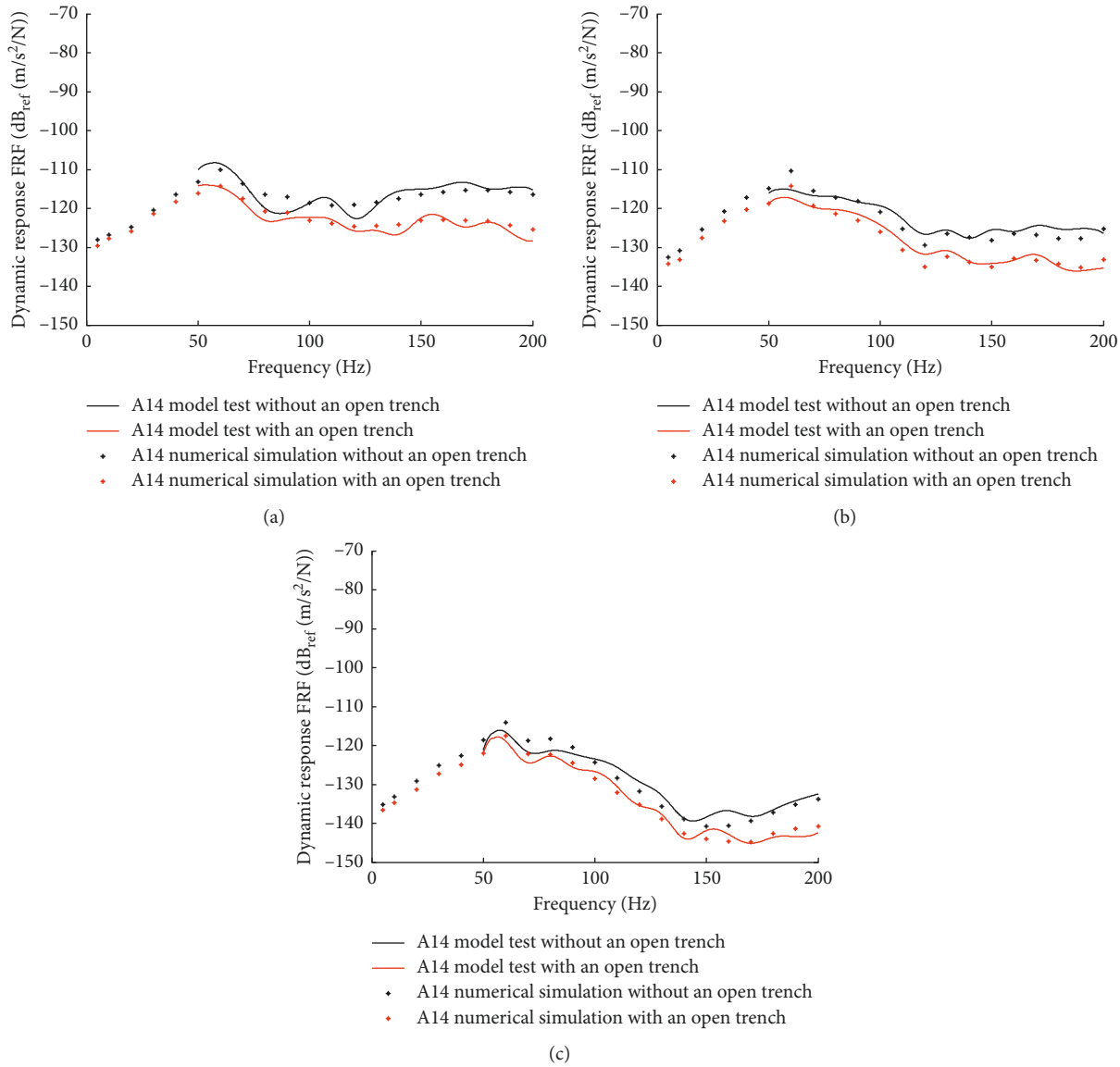

Figure 8: Vertical dynamic response of surface measuring points beyond the trench. (a) Testing point A14. (b) Testing point A16. (c) Testing point A18.

driving system, associated on-board electronics, and heavy machinery located in the laboratory). When the cases with and without the open trench are compared, the FRFs of the vertical dynamic soil responses have similar trends. In the first stage, i.e., before 60 Hz, the FRFs of the three test points (i.e., A14, A16, and A18) increase rapidly as the frequency increases. As 60 Hz is approached, the FRFs decrease as the frequency increases, but there are a few fluctuations. With respect to measuring points A10 and A13, the FRFs increase as the excitation signal increases before reaching the magnitude of 40 Hz. Measuring point A13 is closer to the open trench, and the FRFs obtained from this measuring point fluctuates, i.e., they increase initially, and then they decrease. However, for testing point A10, which is somewhat far away from the open trench, the FRFs increase slowly at first and then decrease.

For the soils beyond the open trench, the effectiveness of the open trench is amplified significantly compared with the soils in front of the open trench. The maximum reduction in amplitude is 13 dB. In addition, the effect increases as the excitation signal increases. The results obtained at testing point A14 indicate that the average difference between the cases with and without the open trench is only 1.6 dB when the frequency ranges from 5 Hz to 50 Hz. However, the average difference increases to 7.8 dB when the period of the amplitude increases to the range of 150–200 Hz. This is because the velocities of the elastic waves (shear wave, compressional wave, and surface wave) in the soil are constant. The higher excitation frequency causes a shorter wavelength. It is more difficult for the short-wavelength waves to go over the isolation trench. Therefore, the higher the frequency of the excitation load is, the better the isolation performance becomes. In addition, the effectiveness of the open trench decreases gradually as its distance from the vibration source increases. An average difference of 5.9 dB is obtained at testing

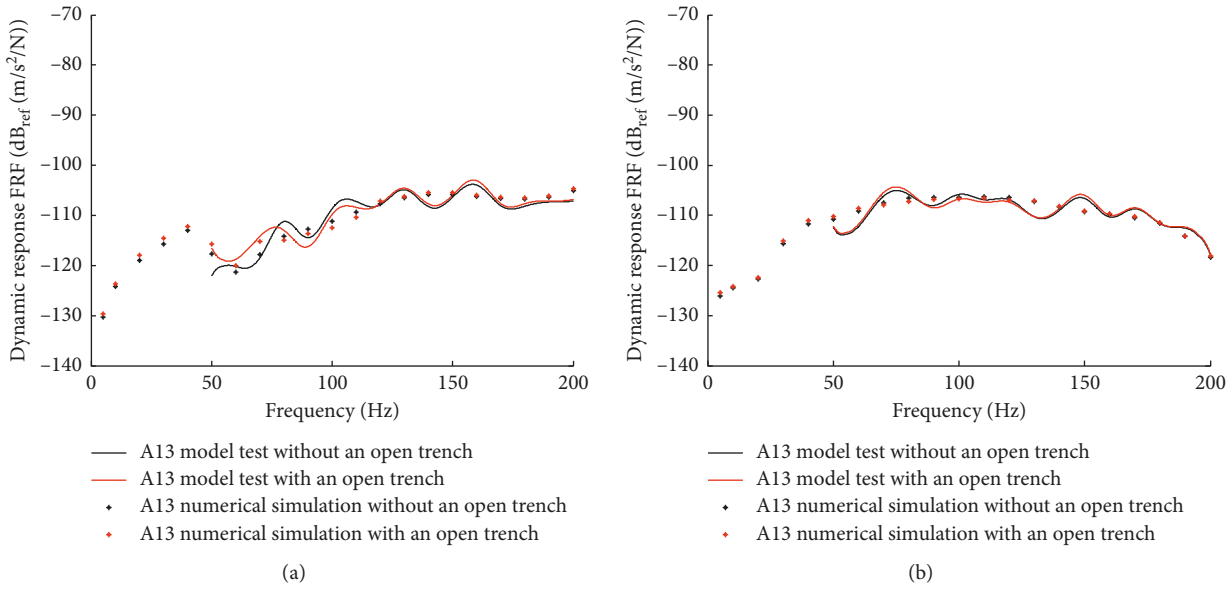

Figure 9: Vertical dynamic response of surface measuring points in front of the open trench. (a) Testing point A13. (b) Testing point A10.

point A16, where there is 14% attenuation compared to that obtained at A14. There is a 29% reduction in the average difference for A18 (4.9 dB) compared to A14. For frequencies in the range of 50–80 Hz, the response of the soil at A13 is amplified when the open trench is used. The highest amplitude value observed is 2.6 dB, and the reason for this observation is that the vibration is reflected at the boundary of the open trench. Due to the superposition of these reflected waves and the incident waves, the dynamic response of the soil in front of the open trench is amplified. However, the open trench has negligible effect on the dynamic response of A10, which is far from the trench.

4.3. Dynamic Response of Soils to Train-Induced Vibration Loading. We have used the train-induced vibration loading in terms of track spectrum level 5, i.e., when the speed of the subway train is 60 km/h. The vertical accelerations are plotted to analyse the effectiveness of the open trench on the dynamic vertical responses of the soil based on the time domain analysis. Figure 10 shows the vertical acceleration responses that are obtained from the surface testing points, and they are characterised by a cycle effect that corresponds to the wheel-set of the subway trains. When the wheel-set passes by the testing points, the vertical acceleration responses increase rapidly. However, when the wheel-set moves away from the measuring points, the vertical acceleration responses exhibit a transient reduction. The VAPs obtained for the cases with an open trench show obvious reductions compared to those obtained without the open trench.

For testing points beyond the open trench, a more significant attenuation of the response of the soil is observed as the distance from the source of the vibration increases. For example, the maximum attenuation at testing point A4 is 28%, but it is 41% for testing point A14. With respect to soils in front of the open trench, the VAPs show very few increases. When the open trench is applied, the VAP is increased by 13% for testing point A13. Obviously, for the soils in front of the open trench, the inclusion of open trenches effectively isolates the subway train-induced vibrations. However, the vibrations are amplified when open trenches are used.

4.4. Parametric Studies of the Open Trenches. To have a better understanding of the isolation performance of open trenches, parametric studies are performed by means of numerical simulations. Open trenches with different widths (0.5, 1, and 2 m), different depths (6, 12, and 18 m), and different distances from the sources of vibration (5, 9, and 13 m) are examined. Table 5 provides the details. The peak vertical acceleration of the particles of soil on the surface of the ground due to the loads of the trains is calculated. In this paper, the insertion loss is used to examine the results in order to gain better insight concerning the test data. The insertion loss is calculated by the following formula:

$$\mathrm{IL} = 20 \log_{10} \frac{a}{a_0}, \tag{4}$$

where IL is the insertion loss, a is the peak vertical acceleration of the particles at the surface of the soil with an open trench, a_0 is the peak vertical acceleration of the particles at the surface of the soil without an open trench.

Figure 11 shows the insertion loss of the response of the soil at the surface of the ground. Figure 11(a) shows that an open trench can effectively reduce the response of the soil behind the trenches. However, the width of open trenches has a relatively small effect on the isolation performance of an open trench. As the width of the trench is increased, the response of the soil is reduced slightly. The average reductions in the amplitudes of the soil's dynamic response

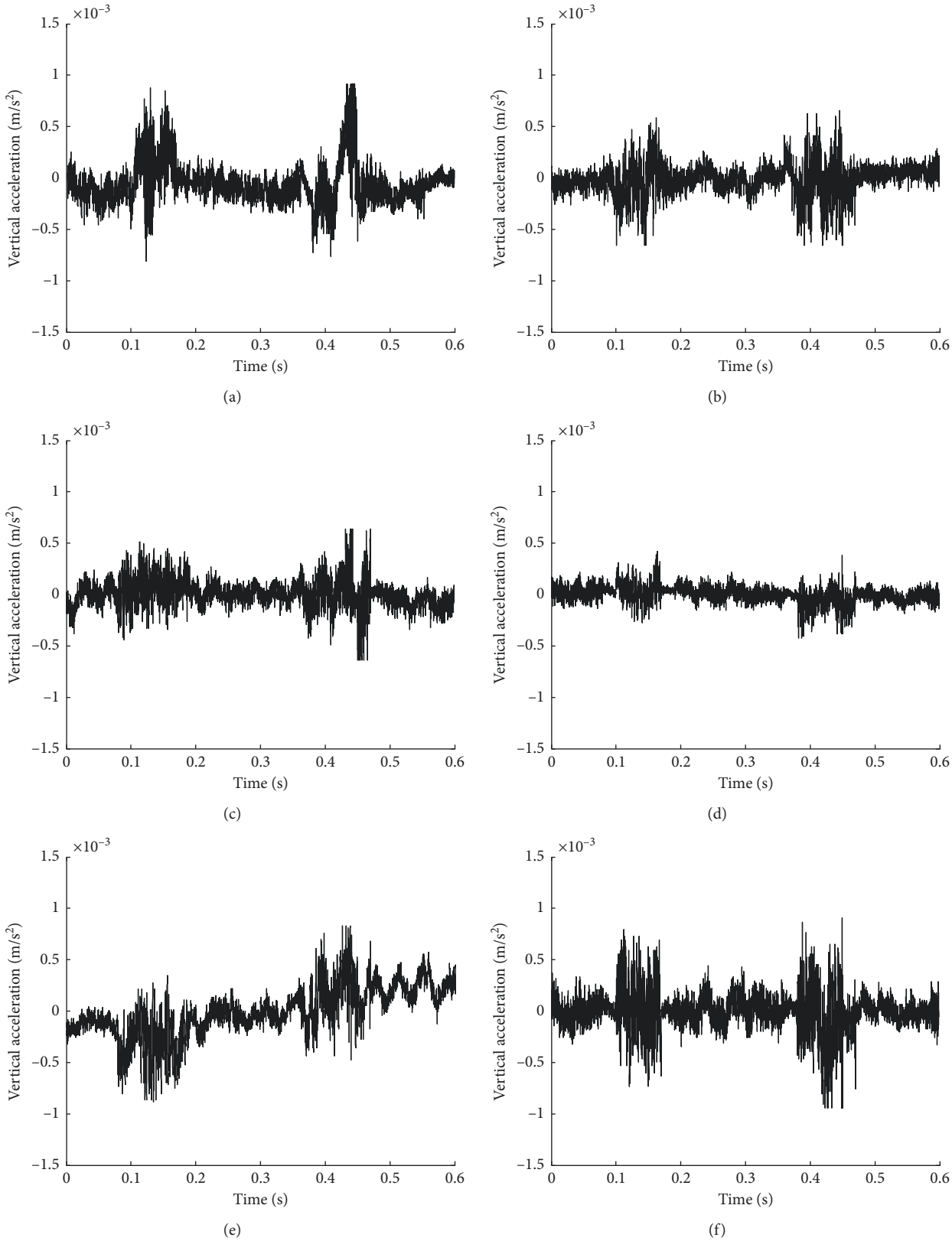

Figure 10: Vertical dynamic response of soil under train-induced vibration load. (a) Testing point A4 without an open trench. (b) Testing point A4 with an open trench. (c) Testing point A14 without an open trench. (d) Testing point A14 with an open trench. (e) Testing point A13 without an open trench. (f) Testing point A13 with an open trench.

Table 5: Numerical simulation cases.

Case	Purpose of analyses	Depth, h (m)	Width, w (m)	Distance, d (m)	Type of isolation trench
1	Trench width	18	0.5, 1, 2	9	Open trench
2	Trench depth	6, 12, 18	2	9	Open trench
3	Trench position	18	2	5, 9, 13	Open trench

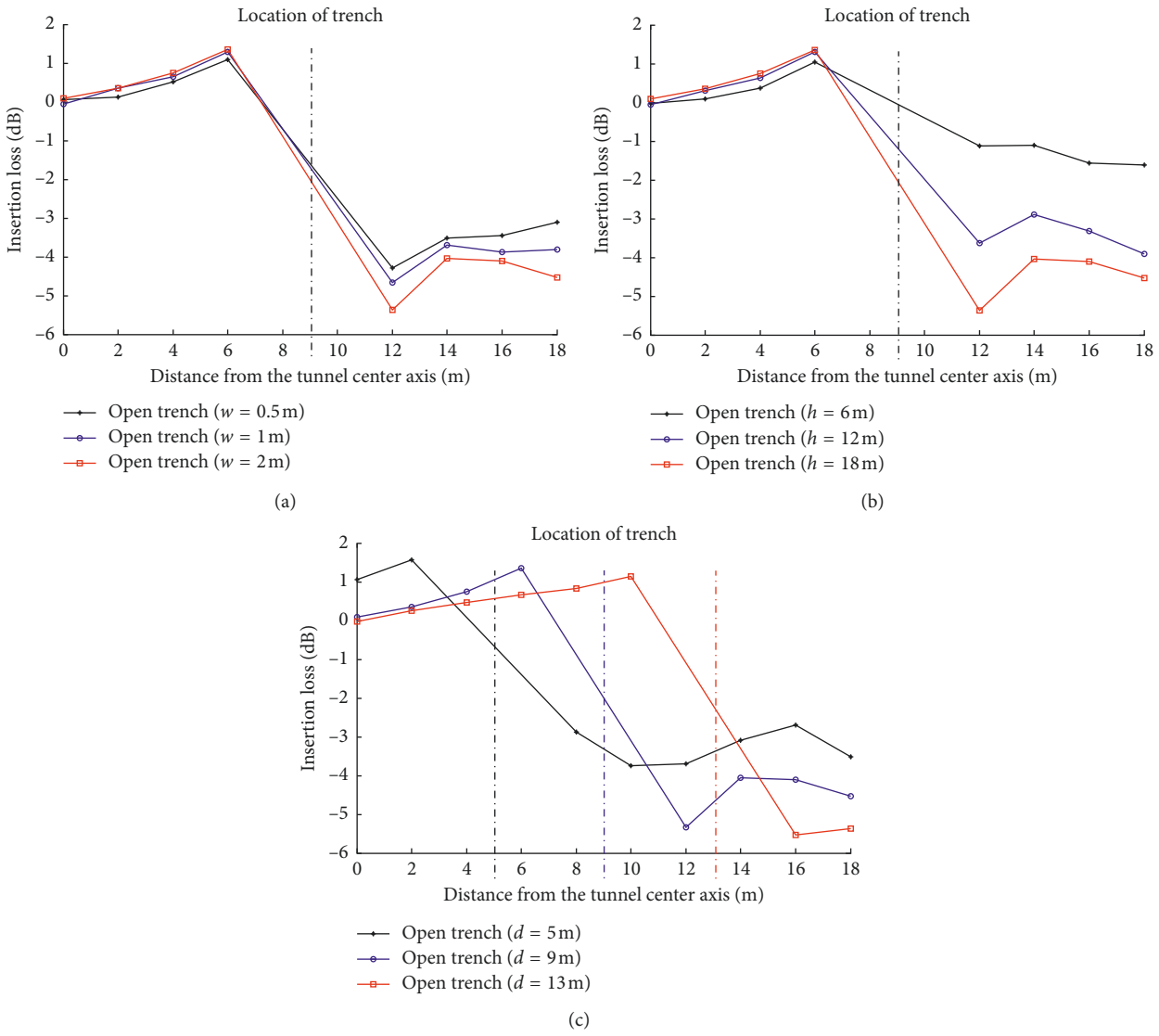

Figure 11: Insertion loss at the surface of the ground. (a) Different trench widths. (b) Different trench depths. (c) Different trench positions.

behind the trenches with widths of 0.5, 1.0, and 2.0 m are 3.6, 3.7, and 4.2 dB, respectively. The phenomenon of amplifying the response of the soil in front of the trench is not affected by increases in the width of the trench.

Figure 11(b) shows that depth of the trench is a critical parameter for the trench isolation performance. The depth of the trench shows relatively small effects on the dynamic response of the soil in front of an open trench. However, the depth of the trench has a significant impact on its isolation performance. The dynamic response of the soil behind the trench is affected mostly by the depth of the trench. With an increase in the trench depth, a clear improvement of isolation performance is observed. At three different trench depths, i.e., 6, 12, and 19 m, the reductions of the soil response behind the trench are 1.3, 3.2, and 4.2 dB, respectively. These results suggest that a deep trench should be used to obtain a better reduction of the vibration.

Figure 11(c) shows the effects of the location of the trench on the isolation performance. The amplification of the response of the soil in front of the trench is more obvious, when the trench is closer to the source of the vibration. As the distance from the trench to tunnel is decreased, the peak response in front of the trenches

increases slightly. A better reduction of vibration occurs when the trench is closer to the measurement points. For example, at the measurement point A17 (16 m away from the centre of the tunnel), the decreases of soil responses for three different locations of the trenches (i.e., 5, 9, and 13 m) are 2.7, 4.1, and 5.5 dB, respectively.

5. Concluding Remarks

Both physical modelling and numerical simulations were performed to analyse the isolation performance of open trenches on the subway train-induced vibrations. The conclusions can be drawn as below:

(i) Experimental and numerical results were compared for cases with or without an open trench subjected to different vibration loads. In the time and frequency domains, the experimental and numerical simulation results of the vertical dynamic responses demonstrated a reasonably good match, with the difference being within 5 dB.

(ii) The open trench demonstrated a significant isolation effect on the vertical dynamic responses of soils beyond the open trench. According to the sweep testing results, the attenuation of the FRFs was amplified as the excitation frequency increased. The maximum reduction of the soil's response was up to 13 dB. The vertical dynamic responses for the ground soils in front of the open trench were amplified, due to the interactions of the incident and reflected waves. It is concluded that the open trench was an effective isolation technique that can reduce the vibrations induced by a subway train.

(iii) A parametric study was performed in terms of numerical simulations. The effects of depths, widths, and locations of trenches on the isolation performance were determined. The results showed that the width of the trench demonstrated negligible effects on the dynamic response of the soil on the surface of the ground. However, increasing the depth of open trenches could significantly improve their isolation performances. In addition, a better reduction of the vibration was observed when the trench was closer to the measurement points.

Data Availability

The data used to support the findings of this study are available from the corresponding author upon request.

Conflicts of Interest

The authors declare that they have no conflicts of interest.

Acknowledgments

This work was supported by the National Natural Science Foundation of China (Grant nos. 51678499, 51609204, and 51608454), the Fundamental Research Funds for the Central Universities (Grant nos. 2682015CX092 and 2682016CX084) and Ningbo Natural Science Foundation (Grant no. 2018A610350).

References

[1] W.-B. Yang, L.-G. Li, Y.-C. Shang et al., "An experimental study of the dynamic response of shield tunnels under long-term train loads," *Tunnelling and Underground Space Technology*, vol. 79, pp. 67–75, 2018.

[2] J. Lang, "Ground-borne vibrations caused by trams, and control measures," *Journal of Sound and Vibration*, vol. 120, no. 2, pp. 407–412, 1988.

[3] S.-E. Kattis, D. Polyzos, and D.-E. Beskos, "Modelling of pile wave barriers by effective trenches and their screening effectiveness," *Soil Dynamics and Earthquake Engineering*, vol. 18, no. 1, pp. 1–10, 1999.

[4] Y. Dere, "Effectiveness of the floating slab track system constructed at Konya Light Rail," *Measurement*, vol. 89, pp. 48–54, 2016.

[5] G.-Y. Ding, J.-L. Wu, J. Wang, and X.-Q. Hu, "Effect of sand bags on vibration reduction in road subgrade," *Soil Dynamics and Earthquake Engineering*, vol. 100, pp. 529–537, 2017.

[6] E. Çelebi and O. Kırtel, "Non-linear 2-D FE modeling for prediction of screening performance of thin-walled trench barriers in mitigation of train-induced ground vibrations," *Construction and Building Materials*, vol. 42, no. 9, pp. 122–131, 2013.

[7] P. Persson, K. Persson, and G. Sandberg, "Numerical study of reduction in ground vibrations by using barriers," *Engineering Structures*, vol. 115, pp. 18–27, 2016.

[8] M. Adam and O. von Estorff, "Reduction of train-induced building vibrations by using open and filled trenches," *Computers and Structures*, vol. 83, no. 1, pp. 11–24, 2005.

[9] D.-E. Beskos, B. Dasgupta, and I.-G. Vardoulakis, "Vibration isolation using open or filled trenches, Part 1: 2-D homogeneous soil," *Computational Mechanics*, vol. 1, no. 1, pp. 43–63, 1986.

[10] B. Dasgupta, D.-E. Beskos, and I.-G. Vardoulakis, "Vibration isolation using open or filled trenches, part 2: 3-D homogeneous soil," *Computational Mechanics*, vol. 6, no. 2, pp. 129–142, 1990.

[11] K.-L. Leung, D.-E. Beskos, and I.-G. Vardoulakis, "Vibration isolation using open or filled trenches, Part 3: 2-D non homogeneous soil," *Computational Mechanics*, vol. 7, no. 2, pp. 137–148, 1990.

[12] S. Ahmad and T.-M. Al-Hussaini, "Simplified design for vibration screening by open and in-filled trenches," *Journal of Geotechnical Engineering*, vol. 117, no. 1, pp. 67–88, 1991.

[13] S. A. Thau and Y. H. Pao, "Diffractions of horizontal shear waves by a parabolic cylinder and dynamic stress concentrations," *Journal of Applied Mechanics*, vol. 33, no. 4, pp. 785–792, 1966.

[14] J. Lysmer and G. Waas, "Shear waves in plane infinite structures," *Journal of the Engineering Mechanics Division*, vol. 98, pp. 85–105, 1972.

[15] R.-D. Woods, "Screening of Surface Wave in Soils," *Journal of the Soil Mechanics and Foundations Division*, vol. 94, no. 4, pp. 951–979, 1968.

[16] W. A. Haupt, "Surface waves in nonhomogeneous half-space," in *Proceedings of an International Symposium on Dynamical Methods in Soil and Rock Mechanics*, pp. 335–367, Karlsruhe, Germany, 1978.

[17] W.-A. Haupt, "Model tests on screening of surface waves," in *Proceedings of the Tenth International Conference in Soil*

Mechanics and Foundation Engineering, vol. 3, pp. 215–222, Stockholm, Sweden, June 1981.

[18] T.-W. May and B.-A. Bolt, "The effectiveness of trenches in reducing seismic motion," *Earthquake Engineering and Structural Dynamics*, vol. 10, no. 2, pp. 195–210, 2010.

[19] H.-H. Hung, G.-H. Chen, and Y.-B. Yang, "Effect of railway roughness on soil vibrations due to moving trains by 2.5D finite/infinite element approach," *Engineering Structures*, vol. 57, pp. 254–266, 2013.

[20] M. Fuykui and Y. Matsumoto, "Finite difference analysis of Rayleigh wave scatting at a trench," *Bulletin of the Seismological Society of America*, vol. 70, no. 6, pp. 2051–2069, 1980.

[21] O.-C. Zienkiewicz, D.-W. Kelly, and P. Bettess, "The coupling of the finite element method and boundary solution procedures," *International Journal for Numerical Methods in Engineering*, vol. 11, no. 2, pp. 355–375, 2010.

[22] O.-V. Estorff and M.-J. Prabucki, "Dynamic response in the time domain by coupled boundary and finite elements," *Computational Mechanics*, vol. 6, no. 1, pp. 35–46, 1990.

[23] L. Andersen and S.-R.-K. Nielsen, "Reduction of ground vibration by means of barriers or soil improvement along a railway track," *Soil Dynamics and Earthquake Engineering*, vol. 25, no. 7–10, pp. 701–716, 2005.

[24] R. Klein, H. Antes, and D.-L. Houédec, "Efficient 3D modelling of vibration isolation by open trenches," *Computers and Structures*, vol. 64, no. 1–4, pp. 809–817, 1997.

[25] S.-D. Ekanayake, D.-S. Liyanapathirana, and C.-J. Leo, "Attenuation of ground vibrations using in-filled wave barriers," *Soil Dynamics and Earthquake Engineering*, vol. 67, pp. 290–300, 2014.

[26] K.-L. Leung, I.-G. Vardoulakis, D.-E. Beskos, and J.-L. Tassoulas, "Vibration isolation by trenches in continuously nonhomogeneous soil by the BEM," *Soil Dynamics and Earthquake Engineering*, vol. 10, no. 3, pp. 172–179, 2015.

[27] A. Garinei, G. Risitano, and L. Scappaticci, "Experimental evaluation of the efficiency of trenches for the mitigation of train-induced vibrations," *Transportation Research Part D Transport and Environment*, vol. 32, no. 1, pp. 303–315, 2014.

[28] J.-L. Liu, L.-G. Zhang, X.-G. Song, H.-H. Cui, E.-P. Hou, and M. Zhao, "Numerical analysis and model test of vibration reduction by open trench on high-speed railway," *Railway Standard Design*, vol. 61, no. 3, pp. 42–46, 2017.

[29] J.-T. Nelson and H.-J. Saurenman, "State of the Art Review, Prediction and Control of Groundborne Noise and Vibration from Rail Transit Trains," Report Number UMTA-MA-06-0049-83-4, Wilson, Ihrig & Associates, Inc., Oakland, CA, USA, 1983.

[30] E.-E. Ungar and E.-K. Bender, "Vibrations produced in buildings by passage of subway trains; parameter estimation for preliminary design," in *Proceedings of Inter-Noise and Noise-Con Congress and Conference*, Sendai, Japan, 1975.

[31] G. P. Wilson, "Noise and vibration characteristics of high speed transit vehicles," Technology Report, Association of American Railroads, Chicago, IL, USA, 1971.

[32] X. Sheng, C.-J.-C. Jones, and D.-J. Thompson, "Ground vibration generated by a harmonic load moving in a circular tunnel in a layered ground," *Journal of Low Frequency Noise Vibration and Active Control*, vol. 22, no. 2, pp. 83–96, 2003.

[33] D.-J. Thompson, J. Jiang, M.-G.-R. Toward et al., "Reducing railway-induced ground-borne vibration by using open trenches and soft-filled barriers," *Soil Dynamics and Earthquake Engineering*, vol. 88, pp. 45–59, 2016.

[34] D.-Y. Ding, W.-N. Liu, K.-F. Li, W.-B. Wang, and M. Ma, "Experimental study on the transmission characteristics of low frequency vibrations induced by metro operation," *China Railway Science*, vol. 32, no. 2, pp. 20–26, 2011.

[35] J.-G. Chen, H. Xia, S.-L. Chen, and M.-B. Su, "Investigation on running-train-induced ground vibrations near railway," *Engineering Mechanics*, vol. 27, no. 1, pp. 98–103, 2010.

[36] W.-B. Yang, M.-F.-M. Hussein, and A.-M. Marshall, "Centrifuge and numerical modelling of ground-borne vibration from an underground tunnel," *Soil Dynamics and Earthquake Engineering*, vol. 51, no. 8, pp. 23–34, 2013.

[37] J.-A. Forrest and H.-E.-M. Hunt, "A three-dimensional tunnel model for calculation of train-induced ground vibration," *Journal of Sound and Vibration*, vol. 294, no. 4-5, pp. 678–705, 2014.

[38] S. Gupta, M.-F.-M. Hussein, G. Degrande, H.-E.-M. Hunt, and D. Clouteau, "A comparison of two numerical models for the prediction of vibrations from underground railway traffic," *Soil Dynamics and Earthquake Engineering*, vol. 27, no. 7, pp. 608–624, 2007.

[39] T. Real, C. Zamorano, F. Ribes, and J.-I. Real, "Train-induced vibration prediction in tunnels using 2D and 3D FEM models in time domain," *Tunnelling & Underground Space Technology Incorporating Trenchless Technology Research*, vol. 49, pp. 376–383, 2015.

[40] S. Iai, "Similitude for shaking table tests on soil-structure-fluid model in 1g gravitational field," *Soils Found*, vol. 29, no. 1, pp. 105–118, 1989.

[41] S. Iai, T. Tobita, and T. Nakahara, "Generalised scaling relations for dynamic centrifuge tests," *Geotechnique*, vol. 55, no. 5, pp. 355–362, 2005.

[42] C. He, K. Feng, and X. Yang, "Model test on segmental lining of Nanjing Yangtze River Tunnel with super-large cross-section," *Chinese Journal of Rock Mechanics and Engineering*, vol. 26, no. 11, pp. 2260–2269, 2007.

[43] J.-A. Cheney, R.-K. Brown, and N.-R. Dhat, "Modeling free-field conditions in centrifuge models," *Journal of Geotechnical Engineering*, vol. 116, no. 9, pp. 1347–1367, 1990.

[44] R.-Y.-S Pak and B.-B. Guzina, "Dynamic characterization of vertically loaded foundations on granular soils," *Journal of Geotechnical Engineering*, vol. 121, no. 3, pp. 274–286, 1995.

[45] C.-J. Coe, J.-H. Prevost, and R.-H. Scanlan, "Dynamic stress wave reflections/attenuation: earthquake simulation in centrifuge soil models," *Earthquake Engineering and Structural Dynamics*, vol. 13, no. 1, pp. 109–128, 2010.

[46] W.-B. Yang, M.-F.-M. Hussein, and A.-M. Marshall, "Centrifuge and numerical modelling of ground-borne vibration from surface sources," *Soil Dynamics and Earthquake Engineering*, vol. 44, no. 1, pp. 78–89, 2013.

[47] D.-W. Huang, S.-H. Zhou, X.-Z. Wang, H.-B. Liu, and R.-L. Zhang, "Design method for longitudinal segment joints of shield tunnel model," *Chinese Journal of Geotechnical Engineering*, vol. 37, no. 6, pp. 1068–1076, 2015.

[48] W.-B. Yang, Z.-Y. Xu, Z.-Q. Chen, L.-G. Li, Q.-X. Yan, and C. He, "Research on influence of segment joints on dynamic response of shield tunnel and surrounding soft soil due to train induced vibration," *Chinese Journal of Rock Mechanics and Engineering*, vol. 36, no. 8, pp. 1977–1988, 2017.

[49] B. Zhou, "Tunnellingnduced ground displacements in sand", Ph.D. thesis, University of Nottingham, Nottingham, UK,2015.

[50] K. Wei, W.-M. Zhai, and J.-H. Xiao, "Vertical random vibration model for subway shield tunnel in soft soil," *Engineering Mechanics*, vol. 31, no. 6, pp. 117–123, 2014.

[51] W.-M. Zhai, K.-Y. Wang, and C.-B. Cai, "Fundamentals of vehicle–track coupled dynamics," *Vehicle System Dynamics*, vol. 47, no. 11, pp. 1349–1376, 2009.
[52] T. Wang, *Numerical Simulation Method and Engineering Application of FLAC3D——in-Depth Analysis of FLAC3D5.0*, China Architecture & Building Press, Vol. P302, China Architecture & Building Press, Beijing, China, 2015.
[53] ICG, *Itasca FLAC-3D Version 5.0.User's Manual*, ICG, Minneapolis, MN, USA, 2012.
[54] J. Lysmer and R.-L. Kuhlemeyer, "Finite dynamic model for infinite media," *Journal of engineering mechanics*, vol. 95, no. 4, pp. 859–877, 1969.
[55] BS ISO, *Mechanical Vibration—Ground-Borne Noise and Vibration Arising from Rail Systems*, International Organization for Standardization, Geneva, Switzerland, 2005.
[56] K. Ishihara, *Soil Behaviour in Earthquake Geotechnics*, Oxford University, Oxford, UK, 1996.
[57] D.-J. Ewins, *Modal Testing: Theory and Practice*, Research Studies Press, Boston, MA, USA, 1984.
[58] K.-G. McConnell, *Vibration Testing: Theory and Practice*, John Wiley & Sons, Hoboken, NJ, USA, 1995.